scientific reports

Check for updates

OPEN

Modelled broad-scale shifts on seafloor ecosystem functioning due to microplastic impacts on bioturbation

Yuxi You[1]✉, Alice Della Penna[1,2] & Simon Francis Thrush[1]

Bioturbating species play an essential role in regulating nutrient cycling in marine sediments, but their interaction with microplastics (MP) remains poorly understood. Here we investigated the linkage between MP and ecosystem functioning using experimental observations of luminophore distribution in the sediment to parametrize bioturbation coefficients (D_b). this information as fed into a simplified transport-reaction model, allowing us to upscale our experimental results. We found that the composition of bioturbators modulated shifts in the ecosystem functioning under microplastic stress. Maldanid worms (*Macroclymenella stewartensis)*, functionally deep burrowing and upward-conveyor belt feeders, became less active. The D_b of *M. stewartensis* reduced by 25% with the addition of 0.002 g MP cm^{-2} at surface sediment, causing accumulation of organic matter in the oxic sediment zone and stimulating aerobic respiration by 18%. In contract, the tellinid bivalve *Macomona liliana*, functionally a surface -deposit feeder that excretes at depth, maintained particle mixing behaviour in MP-contaminated systems. This study provides a mechanistic insight into the impacts of MP and indicates that the functional role of bioturbating species should be involved in assessing the global impact of MP. The model allowed us to understand the broad-scale impact of MP on seafloor habitat.

Plastics of micro- and nano-size are the most hazardous and wide-spread plastic pollution[1–3], but their ecological impacts involve complex interactions among environmental components that are largely unknown [4,5]. Most microplastics (MP, dia. < 0.5 cm) end up on the seafloor, particularly in coastal sediments[6–9]. Plastic particles deposited in sediment habitats are threatening benthic species. For example, the polychaete *Arenicola marina* suffered a 50% loss of energy reserves with reduced feeding rates when they ingested unplasticized polyvinyl-chloride (UPVC) particles[10]. Green et al. (2016) demonstrated that after one-month exposure *A. marina's* burrowing capacity decreased with increasing dosages of MP (from 0.02%, 0.2%, 2% by wet weight sediment)[11]. The deposit-feeding bivalve *Macomona liliana* lost burrow capacity after 31-day exposure to polyethylene terephthalate microplastics (PET) (1% by sediment weight)[12]. Recent studies found sediment dwellers (e.g., the deposit feeding bivalve *Limecola balthica*) avoids the MP by penetrating deeper to the sediment and reduces their food intakes[13]. These effects on worm and bivalve species lead to changes in their behaviours and potential shifts in ecosystem function roles, notably in bioturbation.

Bioturbation is referred as the movement of sediment particles and porewater by animals: it plays a critical functional role of benthic macrofauna mediating the ecosystem responses and enhances the cycling of carbon and nitrogen in marine environments[14–17]. Bioturbation can take many forms depending on animal body-size, density, feeding and burrowing strategies. These factors affect how animals redistribute particles from the sediment surface to different depths[18,19], influence the sediment erodibility[20,21], determine the heterogeneity of biogenic habitats, and maintain the resilience of ecosystem functions[22,23]. Bioturbation modes also influence how MP transport in the sediments. The conveyor-belt feeders that can transport particles in both up and downward directions might induce a deep penetration of MP in the sediment, while biodiffusors with strict upward conveying mode retain less MP in the deep zone[24]. However, the cumulative effects of MP pollution on bioturbation will depend on the sensitivity of individual species and the specific role they play in the sediment. The loss of large macrofauna and their functional roles can lead to a cascading effect on the ecosystem functioning[25–27]; therefore, the potential for broad-scale shifts in ecosystem functions due to the impact of MP on the macrofauna playing a role as bioturbator needs to be assessed[28,29].

[1]Institute of Marine Science, The University of Auckland, Auckland 1010, New Zealand. [2]School of Biology Science, The University of Auckland, Auckland 1010, New Zealand. ✉email: yyou382@aucklanduni.ac.nz

Here, we upscale the impacts of MP to an ecosystem level by reparametrizing the bioturbation coefficient D_b. D_b is derived from the biological mixing patterns that reflect the response of bioturbators to their environmental conditions (e.g., contamination, sedimentation, food availability)[16,30]. For example, in petrol-contaminated sediments, the benthic infauna community contributed to a peak accumulation of particles 2–4 cm sediment depth[31]. Similarly, the polychaete (*Perinereis adbuhitensis*) lost its deep transporting ability with particle penetration to a depth of 6–8 cm reduced with the increasing concentrations of cadmium and copper[32]. Such observed changes in particle transport profiles are the indicator of pollution stress on infaunal groups.

In transport-reaction models [17,33,34], the bioturbation coefficient (D_b) represents the macrofaunal function role in reworking sediment particles and transferring organic matter (OM) to the microbial community in the sediment as a critical step for OM degradation. The penetrated OM stimulates microbial activities at different sediment zones e.g., aerobic mineralization and denitrification [35–37]. In a simplified sediment system, aerobic mineralization takes place in the oxic zone[34]. The anoxic zone is the central place for multiple reduction processes such as NO_3^- being reduced to NH_4^+ or denitrifying to N_2 [38]; the reduced products from anaerobic processes in turn also enhance denitrification[17]. Potentially, the bioturbation coefficient D_b could mediate the impact of MP to ecosystem functions and allow observations of how MP changes D_b to be upscaled to assess broadscale consequences of MP pollution in marine seafloors.

In this study, we measured D_b in a laboratory experiment investigating the impacts of MP on two large and functionally important species, the maldanid polychaete *Macroclymenella stewartensis* and tellinid bivalve *Macomona liliana*. D_b measurements made under different MP concentrations were then used to parameterize a simplified transport-reaction model[34] (Table S2, supplementary). We choose this model because it provides estimates of organic matter (OM) fluxes down the sediment column. D_b is a key driver of the redistribution of OM influxes and thus the portion of aerobic mineralization in the oxic sediment[34]. This model assumes that, in the oxic zone, the penetrated OM induces equivalent oxygen demands for the complete aerobic degradation. In the anoxic zone, the penetrated OM participates in denitrification processes, and multiple anaerobic processes deliver the reduced components (e.g., NH_4^+, Fe^{2+}, Mn^{2+}, H_2S) to enhance the N-cycling[17,39]. The difference between OM inputs and aerobic mineralization in this virtual ecosystem provides a proxy for reduction processes. Denitrification consumes energy from penetrated OM to regenerate N_2 [17]. In the context of this study, N_2 production is a proxy for reduction processes that omits the complexity of multiple degradation pathways, and it is the source of the N_2 released from sediment–water interface (SWI) (Fig. 1).

Results

Bioturbation coefficient D_b vary in response to changes in MP concentration

In treatments hosting only worms or the combined two species, decreases of D_b compared to the control were 25% with 0.002 g cm^{-2} of MP (Fig. 2; Table 1). The highest D_b value (10.69cm^2 $year^{-1}$) was measured in the worm groups without MP and changes of D_b compared to the control was almost -30% with high concentration level of MP (0.02 g cm^{-2}) (Table 1). Bivalve groups had a relatively stable particle mixing intensity (7.04–7.22 cm^2 $year^{-1}$) in MP treatments. The difference between worm and bivalve groups on D_b values decreased (7.58 cm^2 $year^{-1}$ vs. 7.17 cm^2 $year^{-1}$) when exposed to a higher concentration of MP (0.02 g cm^{-2}).

Concentrations of OM penetrated along sediment depths were determined by D_b from bivalve, combined and worm groups separately (Fig. 3). In worm groups, MP treatments had more OM depositing in the sediment surface (0–2 cm). The group with combined of bivalve and worm had a similar trend. A convergence of OM concentration profiles from bivalve group shows there was no change in OM penetration profiles after adding MP.

Ecosystem functioning in MP-bioturbator groups

Fraction of aerobic mineralization (β) accounting to total OM degradation varied with D_b in the worm-only and combined groups, and this induced changes on oxygen consumption and nitrogen production (Fig. 4; Table 2).

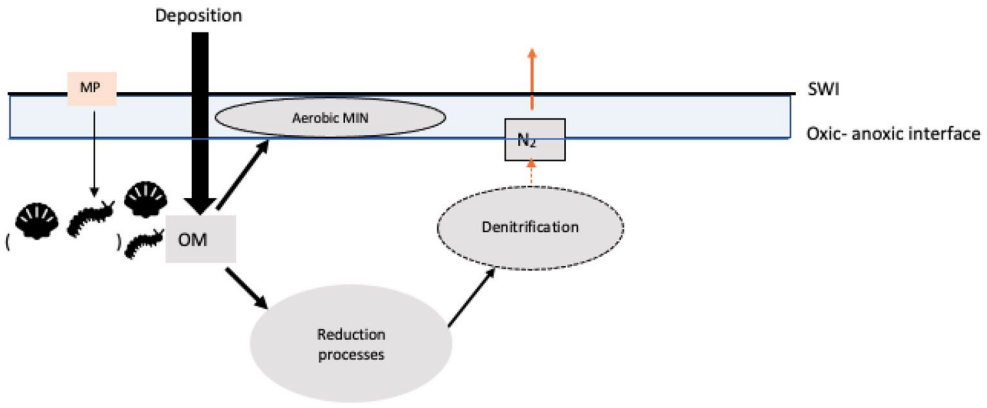

Figure 1. Conceptual simplified diagram of MP interacting with bioturbation and associated processes from OM degradation. *Aerobic MIN* aerobic mineralization; N_2 production is the outcome from denitrification processes (orange arrow). Bivalve and worm symbols imply sediment reworking by these bioturbating species. This diagram is modified from conceptual diagram in Middelburg (2019)[17].

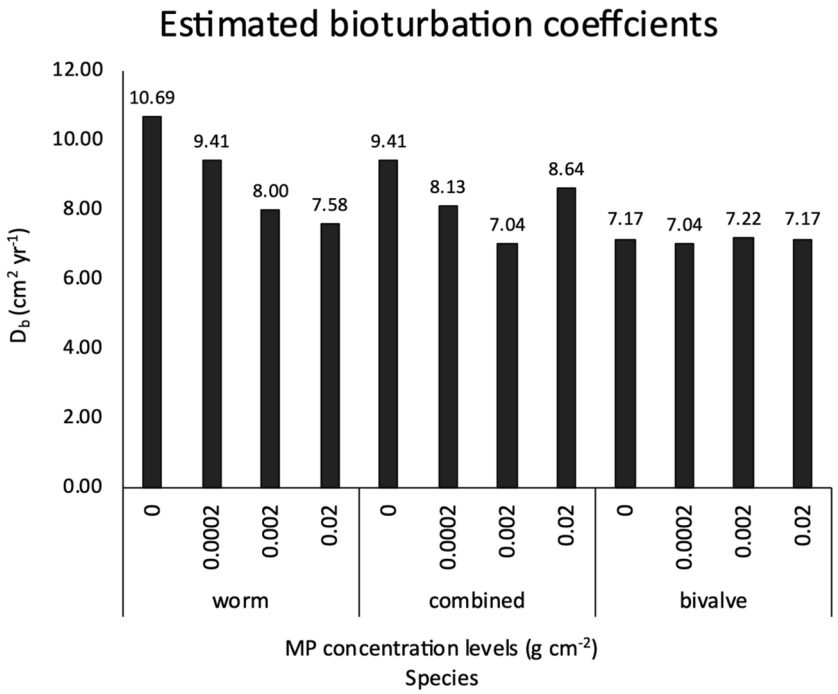

Figure 2. Estimated bioturbation coeffcient D_b (cm^2 year^{-1}) of worm, combined and bivalve groups in MP treatments.

Increases of MP concentrations (g cm^{-2})	Changes (%) of D_b compared to the control		
	Worm (%)	Combined (%)	Bivalve (%)
0.0002	−12	−14	−2
0.002	−25	−25	1
0.02	−29	−8	0

Table 1. Percentage changes of D_b in MP treatment (increased concentration from 0.0002 to 0.02 g cm^{-2}) compared to that in the control.

In the worm groups, aerobic mineralization fraction increased when D_b decreased: the percentage of change of O_2 consumption rates was from 6.58 to 18.73% when MP concentration increased from 0.0002 to 0.02 g cm^{-2} (Fig. 4; Table 2). N_2 production compared to the control decreased from 1.58 to 4.49% at the expense of increased aerobic mineralization. A similar, but weaker trend was in the combined groups: when MP concentration reached 0.002 g cm^{-2}, the O_2 consumption rates compared to the control increased by 15.66%. The fraction of aerobic mineralization β, oxygen consumption rates $F_{\_o2}$ and estimated N_2 production $R_{(N)}$ were invariant in bivalve groups when MP concentration increased.

Discussion

Bioturbation coefficients in MP-contaminated system

We expect that the functional traits of different species, such as the feeding and movement of worms and bivalves determine the responses of the sediment ecosystem to MP pollution. In our study, the highest D_b was observed in experiments occupied by worms without MP and this value decreased as MP concentrations increased, whereas the D_b of bivalves was relatively stable. As a tube builder, the maldanid polychaete *M. stewartensis* feeds head-down around 10 cm depth in the sediment and excretes faeces on the sediment surface[40]. This burrowing mode enlarges turnover areas through sediment columns, increasing the oxygen penetration depth and subducting more labile OM to the deep zone [41,42]. This behaviour can explain higher bioturbation coefficients in the worm groups compared to the bivalve ones. Exposure to MP increases the risk of worms ingesting MP, and this may cause health issues including gut inflammation, reduction of their ingestion rates and energy reserves, suppression of burrowing activities, and limitation to reproduction[10,11]. The D_b values of worms decreased to a level similar to the bivalve's when MP concentration was increased. A reduced bioturbation rate means less sediment turnover scales and particle mixing[43]. While our results imply potential toxic effects of MP on maldanid burrowing behaviour, this is not apparent for the deposit-feeding bivalve (*M. liliana*) which uses a long siphon to capture the food particles at the sediment surface[44]. Previous studies have shown that *M. liliana* are impacted by MP with reduced reburial rates[12,45] which seem to contrast our finding in terms of bioturbation. However,

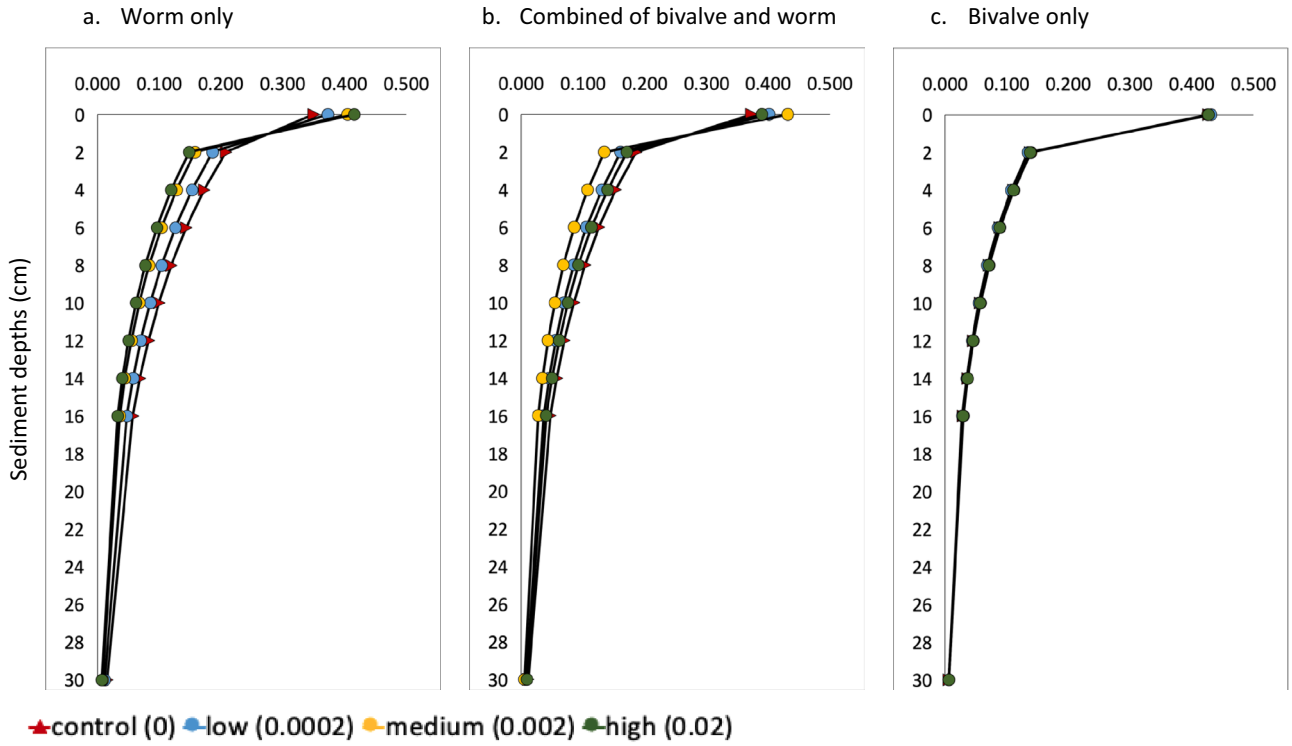

Figure 3. Simulated OM concentrations along sediment depth from species groups (**a**. worm, **b**. combined of bivalve and worm, **c**. bivalve) with concentration levels of MP: 0, 0002, 0.002, 0.02 g cm^{-2}. Note that in (**c**) the four lines overlap.

in this study we focused on particle movement to calculate D_b, whereas the role of *M. liliana* in regulating the nutrient cycling may be more strongly linked to porewater advection and redox oscillations[46]. *M. liliana* periodically pressures overlying fluids and oxygenized-water to the burrowed zone during feeding period[47]. Although the particle reworking intensity of the bivalve group in MP treatments remains stable, it might be because the parameter D_b has limitations in explaining these fluid oscillation behaviours.

MP weakened the particle mixing intensity by maldanid worm and reworking behaviours of tellinid bivalve might dominate the system when MP concentration increased. D_b values from worm groups decreased by the increased concentration of MP; the values from bivalve and combined groups converged to a similar level (7.22, 7.04 cm^2 $year^{-1}$) when MP concentration reached 0.002 g cm^{-2}. Chemical pollution has been reported to reduce the bioturbation potential as a result of the losing species diversity and reduced community biomass[48]. Large and functional important species have dominant impacts on particle redistribution and nutrient cycling as well as the community structure, which is more influential than species diversity[25,27,49]. Bioturbating species take different strategies to adapt to environment stresses (e.g., marine heatwaves, acidification, nutrient loading), with the cascading-effect on ecosystem functioning depends on the functional traits of key species[50–52]. Therefore, feedback from the ecosystem (e.g., nutrient fluxes and oxygen consumption) associated with sediment reworking will depend on the responses from relative dominant species to MP and the specific mechanisms by which they fulfil their individual and collective functional roles. In this study, changes of D_b reflect a potentially different impact of MP on the sediment reworking in the areas dominant with maldanid worm *M. stewartensis* and tellinid bivalve *M. liliana* separately, as well as their transition zones (co-occur of these species) in the seafloor habitats. The bioturbation of *M. liliana* and *M. stewartensis* creates distinct microtopographic features on the sediment surface that influence the nutrient fluxes[53]. In MP-contaminated habitats, the maldanid worm can loss advantage in deep-particle mixing and maintaining the nutrient cycling. Functional traits of *M. liliana* associated with sediment reworking and generation of porewater pressure gradients will lead the ecosystem processes when two species co-occur, and the habitats becomes homogenized regarding the loss of worm's functional roles. This is likely to happen in the natural habitat when the concentration of MP continues to increase. Currently, there is no consistent way to measure MP concentration, and differences from areal concentrations to mass-based concentrations are common. MP concentrations in the field are often variable, sites with concentration spikes are associated with the in-situ breakdown of larger plastic items[9,54,55]. The range of MP used in our treatments reflects both the variation between sites but also the potential extreme values within sites associated with spatial and temporal dynamics[56–58]. Even MP increasing to 0.002 g cm^{-2} is concerning because the similar contamination level was found in field studies[59].

Ecological consequences from MP-contaminated system

Our measurement of D_b under different MP loads combined with the application of the transport-reaction model indicates that in plastic polluted sediments, less organic matter (OM) is subducted deep into the sediment

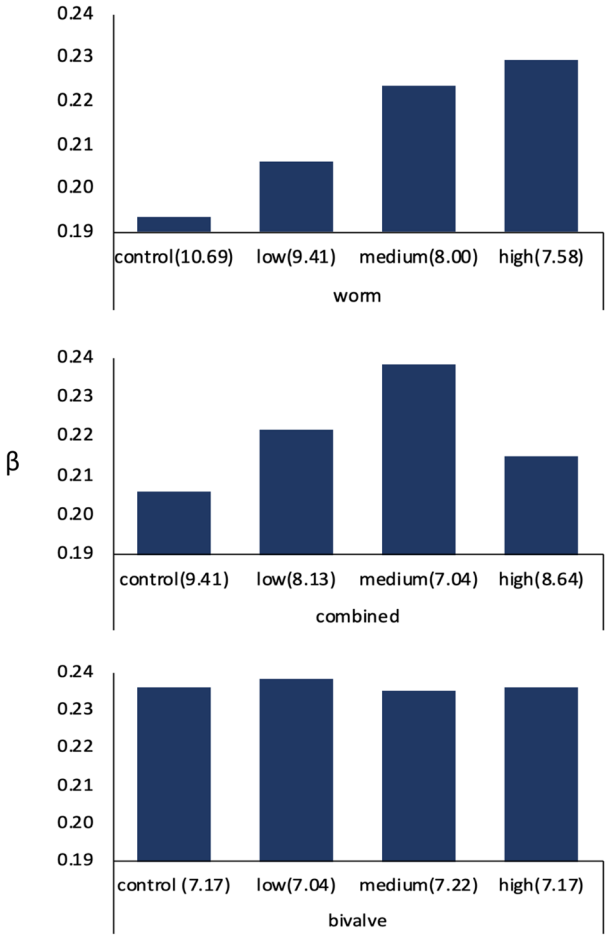

Figure 4. Fraction of aerobic mineralization β at oxic zone in worm, combined and bivalve groups from MP treatments at control, low medium and high levels (D_b values in parenthesis).

Increases of MP concentrations (g cm^{-2})	Changes (%) of oxygen consumption rates (F_{o2}) and [estimated N_2 production ($R_{(N)}$)] compared to the control		
	Worm, % [%]	Combined, % [%]	Bivalve, % [%]
0.0002 (low)	6.58 [−1.58]	7.58 [−1.97]	0.97 [−0.30]
0.002 (medium)	15.64 [−3.75]	15.66 [−4.07]	−0.31 [0.10]
0.02 (high)	18.73 [−4.49]	4.09 [−1.14]	0.00 [0.00]

Table 2. Percentage changes compared to control on oxygen consumption rates (F_{o2}) and estimated N_2 production (values in square brackets) with increases of MP concentrations.

resulting in higher oxygen consumption in the sediment. The associated effects on ecosystem functioning with bioturbations are summarized in Fig. 5.

The shallow penetration of OM stimulates microbial activities in the oxic zone with more oxygen demands for the respiration. Increasing oxygen demands in MP-contaminated sediments were reported in previous laboratory tests[13], and was associated with the reduced burrowing capacity of worms and bivalves with different functional traits to our study species (i.e., *Arenicola marina*, *Cerastoderma glaucum*)[11,13]. The observation from a real-world experiment reveals that mollusc abundance alone cannot explain the increasing oxygen demands in the dark (aerobic respiration), and the linkage of macrofauna and sediment oxygen consumption can be broken with the contamination of fibric microplastic[60]. Our study provides a mechanistic insight into this phenomenon: aerobic-microbial activities consuming OM at the sediment surface may overweigh macrofauna's mediating effects on microbial activities through oxic-anoxic sediment zones. The OM-enriched sediment surface often needs higher oxygen demands and it causes a reduced oxygen penetration depth[61,62]. The long-term persistence of this event, in turn, causes the hypoxia stress on macrofauna assemblages and increases the risk of eutrophication [63,64]. In the intertidal areas, low-density and the removal of large bioturbators (e.g., *M. liliana*, *M. stewartensis* and *A.*

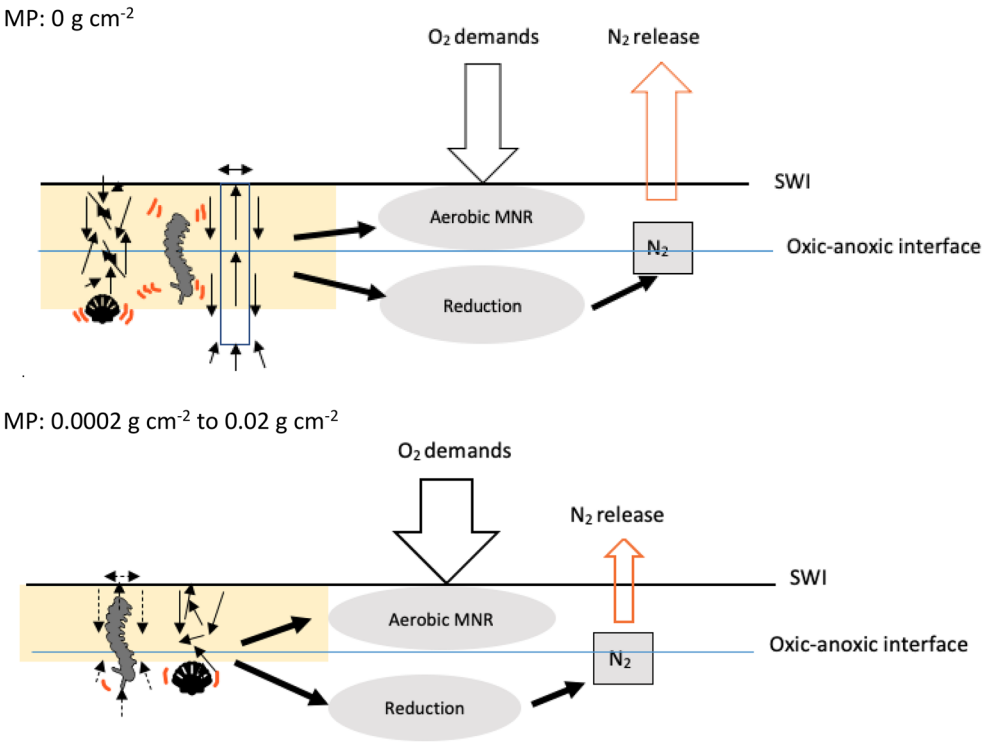

Figure 5. Schematic representation of ecosystem functions in MP- and control seafloor based on the study outputs (modified from Middelburg, 2019[17]). Yellow zone: OM penetration pattern. *SW* sediment–water interface, *aerobic MNR* aerobic mineralization, Reduction: reduction processes at anoxic zone: Bivalve and worm symbols: burrowing patterns of maldanid worm *Macroclymenella stewartensis* and tellinid bivalve *Macomona liliana* (modified from Schenone et al., 2019[40]). N_2: nitrogen production from reduction processes that potentially can release at SWI.

marina) often lead to a lower consumption of carbon sourced from microphytobenthos (MPB) on sediment surface[65,66]. In our study, the shallow penetration of OM also indicates few labile OM resources (e.g., MPB) are transported to the sediment subsurface and incorporated to the nutrient cycling. The composition of MPB shifts the trophic linkage between MPB and macrofauna breaks: macrofauna grazing on microphytes provides nutrients (e.g., ammoniacal nitrogen) to maintain the MPB standing stock[49]. However, MP might break this linkage with increasing cyanobacteria biomass in the MPB community, which changes the nutrient cycling in the sediment[45]. The effect of MP is concerning in these scenarios because the biogeochemical processes that rely on particle mixing by large macrofauna will need a longer time to recover, either as the toxicity of the plastic decreases or as more tolerant species with similar functional traits replace the more sensitive species [67].

Ecological consequences of MP are context-dependent on the species composition and MP properties (e.g., concentrations); therefore, the outputs should be carefully interpreted due to the simplification of the model. Firstly, the parameter D_b may be sensitive to changes in the worm's activities and deep particle mixing patterns, but it does not represent the changes on bivalve's fluid oscillation. The hydraulic activities extend the oxic zones and mediate the microbial activities periodically[47,68,69], and this needs to be involved in the further assessment. Secondly, we have not included responses from microbial community and microphytobenthos to MP. Previous studies have shown MP triggering microbial aggregation[70,71], shifting the microbial compositions [72] and increasing cyanobacteria biomass at the sediment surface [45]. While these effects may be most pronounced in shallow photic sediments, these are common in harbours and estuaries that often exhibit high MP concentrations. We expect that excluding these components might deviate the prediction from the observation in a real-world experiment. For example, the growth of the cyanobacteria at the photic sediment surface will reduce the downward diffusion of O_2 fluxes, and O_2 consumption decreases when gross photosynthesis increases[73]. In this circumstance, the observed O_2 consumption rate from MP treatments can be a net effect of increased aerobic respiration induced by OM accumulation and gross photosynthesis caused by cyanobacteria. Thirdly, the model assumption of complete degradation of OM in a virtual semi-closed sediment zone[34] leads to the analytical estimation of O_2 consumption and N_2 production via feedbacks to metabolic resource redistribution that is tuned by parameter D_b. Although N_2 production in MP-treatments decreased by a small percentage owing to increased aerobic mineralization in worm and combined groups; a weakened nitrogen cycling is likely a result of a chains-reaction when macrofauna loses its functional role in transporting labile OM and regulating microbial activities. This study has not included multiple limiting factors (e.g., OM quality, NO_3^- concentration) in N-cycling, as well as the complexity of pathways of denitrification, including directly denitrifying NO_3^- in overlying water and coupling of nitrification and denitrification processes at an oxic-anoxic sediment interface[74]. MP as synthetic

polymers potentially participates in OM degradation[75], and some materials (PLA) can serve as carbon sources which stimulate both nitrification and denitrification rates[72]. In a eutrophic system, OM (quality and quantity) constrains denitrification when overlying water provides sufficient NO_3^-; in a low-nutrient system, the NO_3^- supply from nitrification is the limiting factor for denitrification in the sediment[74]. In this case, we predicted that when the bioturbation rate decreased because of MP, O_2 demands increased because of OM accumulation. If this phenomenon co-occurs with decreased O_2 penetration depth, the nitrification can stop due to the limited O_2 supply, and this decouples nitrification from denitrification in the sediment. These undefined relationships increase the difficulty in predicting MP's impacts on ecosystem functioning. The relationship between MP and bioturbation needs more empirical data to confirm before upscaling to a global-scale model[76–78].

Conclusion

Our study highlights that the impact of MP on bioturbation can result in broad-scale shifts in ecosystem functioning. These effects are the result of interaction between functional traits of bioturbating species and concentration of MP. The strongest effects on function were driven by changes in the deep-burrowing behaviour of maldanid worms. This result indicates that substantial effects of MP pollution on ecosystem function may be more evident in areas dominated by large deep burrowing species rather than in more degraded ecosystems dominated by other smaller macrofauna[25,49]. The differences in our estimates of D_b from the maldanid worm and the tellinid bivalve highlight the importance of considering the specific mechanisms of bioturbation and how they can be incorporated in biogeochemical models. Linking laboratory observation to the numerical model allows us to estimate the consequences at the ecosystem level of MP contamination. Future studies can expand on both the range of functional traits of key species and consider community level effects as well as considering the hydraulic activities of macrofauna alongside particle transport.

Methods

Measuring D_b under different MP loads

Sediment and animal collection

Sediment and animals, the tellinid bivalve *Macomona liliana*, and the maldanid polychaete *Macroclymenella stewartensis,* were collected during low tide from Whāngateau estuary (36°18′52.37" S, 174°46′17.09" E), New Zealand. Sediments (grain size: 164.94 ± 1.58 µm mean ± standard deviation, fine sand fraction: 55.5%, mud content:11.4%) were sieved through 500 µm mesh a to remove t macrofauna. Bivalve *M. liliana* (minimum shell length: 3.8 cm, maximum shell length: 4cm) and worm *M. stewartensis* (body length: ~ 10 cm) were hand-collected from their habitats. The estimated wet weights for bivalve and worm at these sizes were 2.3 g and 0.2 g, respectively [40].

MP preparation

Prewashed polypropylene plastic pellets (PP, diameter: 4 mm, LINGS limited, China) were frozen for 2 weeks at −80 °C to embrittle the PP particles. The frozen raw materials were ground using a coffee mill (Coffee tech Limited, New Zealand). MP particles (hereafter: MP) were sieved through 500 µm mesh to control the size of MP (diameter < 500 µm).

Preincubation

Before being combined with target species, MP were introduced to the top 1 cm surface sediment and incubated from 30th May to 17th, June, 2022. This step is designed to reduce the resuspension of MP. A 2-week incubation allows microalgae to cover the surface of MP [79]. This bio-stabilization (e.g., growth of biofilm and interact with microalgae) on the sediment bed is the precondition for MP deposition in the sediment [6].

Preserved MP and surface sediment were homogenized and incubated in individual containers (1cm depth, surface areas: 727.8 cm^2). We created a gradient in MP concentrations with values of 0.02, 0.002, 0.0002 g cm^{-2} by surface areas of sediment. Sediments without plastic addition were incubated as a control. Each control and MP treatment was replicated three times, with three blocks of sediment allocated in each container. These preincubated sediments were set up at temperature at ~ 16 °C, and topped up with filtered, clean seawater. A gentle inflow rate ~ 35 ml min^{-1} was set to limit resuspension in the sediment columns. All MP treatments were randomly layout under four double Aqua One Reflector Fluroglow T8 (40 W) sunlight tubes hung 55 cm above the water surface, and set on a 12 h light/dark cycle. The photosynthetic photon flux density (PAR, waveband 400–700 nm) on the surface of incubated water was measured by Li-Cor LI-190R quantum sensor coupled with a Li-Cor data-logger (Li-Cor, USA), with avg. 165.42 ± SD 5.60 µmol photons m^{-2} s^{-1}. External light was excluded by a blackout curtain.

Main incubation

We measured the sediment reworking profiles from incubations with worms, bivalves, and a combination of the two in MP-contaminated sediment. A total of 36 cylindric buckets (volume: 5 L, height: 24.5 cm) were submerged in the filtered water flow for at least 3 weeks to reduce the release of the plasticizers. All buckets were filled with 11cm clean sieved-sediment and topped with 1 cm surface sediment (surface areas: 240.6 cm^2) from the pre-incubation step. These sediments were settled for 24 h and placed in a bath of sand-filtered seawater (salinity: 35.5, temperature: 16 °C, flow rate: ~ 80 ml min^{-1}, water depth: 13 cm). Healthy worms and bivalves were placed on the surface sediment and allowed to burrow into the sediment and acclimate for 24 h. The main incubation started with no worms or bivalves on the sediment surface. A total of 34 g of luminophores (florescence painted natural sands, grain size diameter: 149.15 µm ± 0.51 mean ± standard deviation) were evenly spread through the water column to cover the surface sediment at a density of 0.14 g luminophores cm^{-2} in the top 1 cm sediment. A control (0 g MP cm^{-2}) and three MP concentration levels (g cm^{-2} surface areas of 1cm depth wet sediment)

were used: (1) low concentration (0.0002 g cm^{-2}), (2) medium concentration (0.002 g cm^{-2}) and (3) high concentration (0.02 g cm^{-2}). These were crossed with three animal treatments (a) two *M. liliana* ('bivalve'), (b) two *M. stewartensis* ('worm') and (c) one *M. liliana* with one *M. stewartensis* ('combined'). The density of two species in each treatment was 83.3 ind. m^{-2} and it is within the ranges of natural density in the habitat [80]. The two species naturally co-occur in New Zealand intertidal soft sediment[40]. These treatments were replicated three times and incubated from 18th June to 12th July in Leigh marine laboratory, The University of Auckland, New Zealand. Incubation buckets were randomly distributed under the same light condition as that in the preincubation step.

Luminophore—sediment sampling

Three sediment cores (10 cm depths, diameter: 2.7 cm) were collected from each bucket. At the end of incubation, the absence of luminophore tracers from the surface sediment are the result of animal burrowing and feeding [81]. Sediment cores were collected from these spots, and sliced into 2 cm increments as five subsamples and pooled from individual buckets.

Luminophore recovery

Subsamples were stirred for 1 h and digested by 15% H_2O_2 solution for 1 week in clean glass beakers to remove organic matter [82]. The digested subsamples were carefully rinsed through distilled water, placed in dust-free containers (70 ml), and freeze-dried for 72 h. Freeze-dried subsamples were weighed and homogenized. Visible shell fragments were picked out from the containers. A cohesive tape (size: 4.0 cm × 4.2 cm, transparent) was vertically inserted to the container and vortexed for 60 s (800 rpm) to homogenize all particles on the tape. The tape covered by luminophores and sediment particles was removed from the container and preserved in petri dishes, and the remaining sediment was re-weighed. The difference on the sample weight was the weight of the particles that attached on the cohesive tape (g). Triplicated tape samples were extracted from each container.

The amount of the luminophores spreads through sediment section (0–2 cm, 2–4 cm, 4–6 cm, 6–8 cm and 8–10 cm depths) reflects the vertical sediment mixing by bioturbation for the luminophore particle[83,84]. Luminophore particles in the tape samples were photographed in a UV light chamber (34 × 26 × 30 cm), with four installed ultraviolet (UV) lights at top corners to deliver consistent illumination. Tape samples were horizontally laid on the bench within the chamber, under a 12 cm distance from camera lens (48-mega pixels, 25× zoom-in). Sample photographs (3024 × 4032 pixels) were binarized as black and white (0: pixels in black areas, 1: pixels in florescent areas) and luminophore particles were calculated by Image J 1.53a (Plugins, Blob labeler). The profiles of luminophore tracers from the laboratory test represents the sediment reworking by bioturbators interacting with MP ($F_{24,180} = 39.037$, $p = 0.000$, 3-way ANOVA test, See Table S1, Supplementary); These observations were fitting to the deterministic bioturbation model (details as below).

Derived D_b by fitting sediment reworking profiles

The observed profiles of luminophore particles from the experiment were fitted to a deterministic bioturbation model to derived the bioturbation coefficients D_b [77,85]. This method has been applied in previous studies[16,81].

The predicted luminophore transportation at each depth was calculated as:

$$Lum(x) = \left(\frac{1}{\sqrt{\pi D_b t}}\right) e^{-x^2/4D_b t} \tag{1}$$

where:

$$\frac{\partial Lum(x)}{\partial x} = 0, \quad when \quad x = 0$$

$$Lum(x \to \infty, t) = 0;$$

D_b is assumed to be consistent in time; t is the duration of the experimental days, 21 days; x is the sediment layers 0–2, 2–4, 4–6, 6–8, 8–10 cm (nominal depths: 0, 2, 4, 6, 8 cm); Lum(x) is the luminophore particles at depth x; D_b was derived from a convergent iteration and the weighted regression of least-squares comparison between the observational (*obs_i*) and predicted luminophore particle (*pred_i*) profiles (see profile example in Fig. 6) using the least square non-linear function (LSQNONLIN, Matlab, 2021b).

The iteration continued until observational data has minimum distance to prediction, resulting in the smallest residual values.

$$\text{Residuals} = \sum_{i=1}^{n} \frac{(obs\_i - pred\_i)^2}{obs_i + 1} \tag{2}$$

Residual outputs have shown the fit of the predicted values to the observational data (see Fig. S2).

Estimated impacts on ecosystem functions by fitting D_b

The simplified transport-reaction model[34] was applied to evaluate the ecosystem functioning associated to bioturbation in MP-contaminated system (parameters and constant values as shown in Table S2). We set a depth of 2 cm sediment as the boundary of oxic zone for aerobic mineralization (Z_{o2}) which is in line to a common range of redox potential layer in the sediment[86]. OM burial was considered negligible due to the dominance of bioturbation[34].

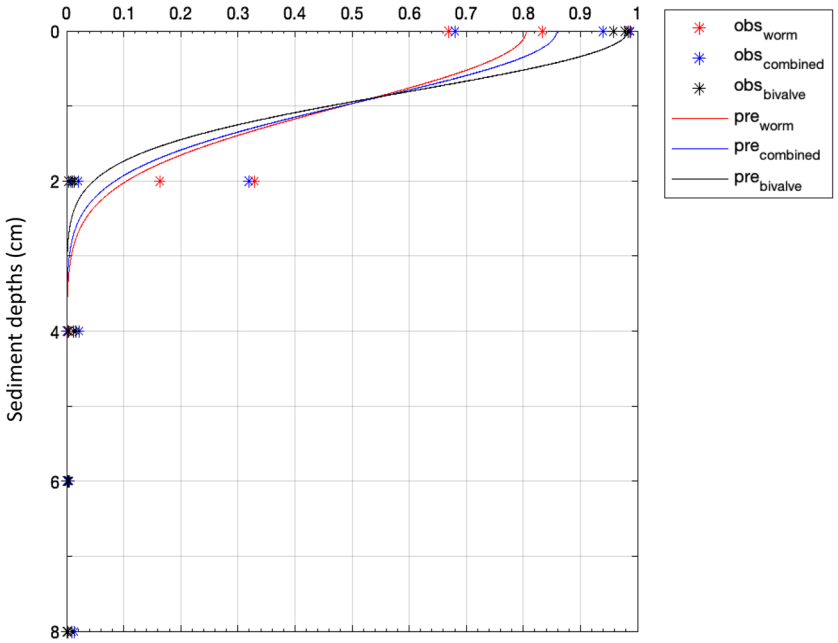

Figure 6. Examples of fitting the observational luminphore profiles (obs_i) to the prediction (pre_i) from bioturbation model to derive the value of D_b from maldanid worm, combined and tellinid bivalve groups in control. Other profiles from MP treatments are in Fig. S1, supplementary.

The profile of OM concentration along sediment depth (C(x), mmol OM g^{-1}):

$$C(x) = C^0 e^{(-x/z)}; \tag{3}$$

where Z is the effective zone of bioturbation:

$$Z = \frac{2D_b}{-\omega + \sqrt{\omega^2 + 4D_b k}}; \tag{4}$$

And the estimated OM concentration (C^0, mmol OM g^{-1}) initially received from sediment–water interface (SWI) is:

$$C^0 = \frac{2F\_OM}{\rho(1-\phi)[\omega + \sqrt{\omega^2 + 4D_b k}]}; \tag{5}$$

The aerobic mineralization rate ($R_{(oxic\_Db),}$ mmol OM cm^{-2} $year^{-1}$) at oxic zone:

$$R(oxic\_D_b) = Z_{o2}k * \rho(1-\phi) * C_{avg}(D_b) = Z_{o2}k\frac{F\_OM}{D_b k}; \tag{6}$$

where $C_{avg}(D_b)$ is the approximate average OM concentration in the oxic zone when D_b dominants the advective transport ($\omega = 0$):

$$C_{avg}(D_b) = \frac{F\_OM}{\rho(1-\phi)\sqrt{D_b k}}; \tag{7}$$

The oxygen consumption rates (mmol cm^{-2} $year^{-1}$) for aerobic mineralization:

$$F_{\_o2} \approx R(oxic\_D_b); \tag{8}$$

The fraction of aerobic mineralization (β) accounting to OM degradation:

$$\beta = \frac{R_{(oxic\_Db)}}{F\_OM} = \frac{Z_{O2}k\frac{F_{OM}}{\sqrt{D_b k}}}{F\_OM} = Z_{O2} * \sqrt{\frac{k}{D_b}}; \tag{9}$$

The fraction of OM fluxes for reduction processes that can enhance denitrification ($R_{(N)}$) :

$$R_{(N)} \cong F\_OM - R_{(oxic\_D_b)} = F\_OM * (1-\beta) \tag{10}$$

$F_{\_OM}$ is a fixed organic matter flux delivered to SWI as a boundary condition, average 0.6 mmol cm^{-2} $year^{-1}$ in coastal environment; k is the organic matter decay constant ($year^{-1}$), k = 0.1; ω is the advective velocity for solids and solutes, 0.1 cm $year^{-1}$; ρ is the sediment density, 2.55 g cm^{-3}; ϕ is the porosity, 0.35.

Data availability

Supplementary contains all relevant data as attached.

Received: 16 June 2023; Accepted: 8 October 2023
Published online: 10 October 2023

References

1. Law, K. L. & Thompson, R. C. Microplastics in the seas. *Science (80-)* **345**, 144–145 (2014).
2. Barnes, D. K. A., Galgani, F., Thompson, R. C. & Barlaz, M. Accumulation and fragmentation of plastic debris in global environments. *Philos. Trans. R Soc. B Biol. Sci.* **364**, 1985–1998 (2009).
3. Chenillat, F., Huck, T., Maes, C., Grima, N. & Blanke, B. Fate of floating plastic debris released along the coasts in a global ocean model. *Mar. Pollut. Bull.* **165**, 112116 (2021).
4. Ockenden, A., Tremblay, L. A., Dikareva, N. & Simon, K. S. Towards more ecologically relevant investigations of the impacts of microplastic pollution in freshwater ecosystems. *Sci. Total Environ.* **792**, 148507 (2021).
5. Yokota, K. *et al.* Finding the missing piece of the aquatic plastic pollution puzzle: Interaction between primary producers and microplastics. *Limnol. Oceanogr. Lett.* **2**, 91–104 (2017).
6. Hope, J. A., Coco, G., Parsons, D. R. & Thrush, S. F. Microplastics interact with benthic biostabilization processes. *Environ. Res. Lett.* **16**, 124058 (2021).
7. Kane, I. A. *et al.* Seafloor microplastic hotspots controlled by deep-sea circulation. *Science (80-)* **368**, 1140–1145 (2020).
8. Napper, I. E. & Thompson, R. C. Release of synthetic microplastic plastic fibres from domestic washing machines: Effects of fabric type and washing conditions. *Mar. Pollut. Bull.* **112**, 39–45 (2016).
9. Turner, A. & Holmes, L. Occurrence, distribution and characteristics of beached plastic production pellets on the island of Malta (central Mediterranean). *Mar. Pollut. Bull.* **62**, 377–381 (2011).
10. Wright, S. L., Rowe, D., Thompson, R. C. & Galloway, T. S. Microplastic ingestion decreases energy reserves in marine worms. *Curr. Biol.* **23**, R1031–R1033 (2013).
11. Green, D. S., Boots, B., Sigwart, J., Jiang, S. & Rocha, C. Effects of conventional and biodegradable microplastics on a marine ecosystem engineer (*Arenicola marina*) and sediment nutrient cycling. *Environ. Pollut.* **208**, 426–434 (2016).
12. You, Y., Thrush, S. F. & Hope, J. A. The impacts of polyethylene terephthalate microplastics (mPETs) on ecosystem functionality in marine sediment. *Mar. Pollut. Bull.* **160**, 111624 (2020).
13. Urban-Malinga, B., Jakubowska, M. & Białowąs, M. Response of sediment-dwelling bivalves to microplastics and its potential implications for benthic processes. *Sci. Total Environ.* **769**, 144302 (2021).
14. Soetaert, K. *et al.* Modeling 210Pb-derived mixing activity in ocean margin sediments: Diffusive versus nonlocal mixing. *J. Mar. Res.* **54**, 1207–1227 (1996).
15. Meysman, F. J. R., Boudreau, B. P. & Middelburg, J. J. Relations between local, nonlocal, discrete and continuous models of bioturbation. *J. Mar. Res.* **61**, 391–410 (2003).
16. Maire, O., Duchêne, J. C., Rosenberg, R., De Mendonça, J. B. & Grémare, A. Effects of food availability on sediment reworking in *Abra ovata* and *A. nitida*. *Mar. Ecol. Prog. Ser.* **319**, 135–153 (2006).
17. Middelburg, J. J. Marine carbon biogeochemistry: A primer for earth system scientists. *Springer Briefs Earth Syst. Sci.* https://doi.org/10.1007/978-3-030-10822-9 (2019).
18. Michaud, E., Desrosiers, G., Mermillod-Blondin, F., Sundby, B. & Stora, G. The functional group approach to bioturbation: The effects of biodiffusers and gallery-diffusers of the *Macoma balthica* community on sediment oxygen uptake. *J. Exp. Mar. Biol. Ecol.* **326**, 77–88 (2005).
19. Michaud, E., Desrosiers, G., Mermillod-Blondin, F., Sundby, B. & Stora, G. The functional group approach to bioturbation: II. The effects of the *Macoma balthica* community on fluxes of nutrients and dissolved organic carbon across the sediment-water interface. *J. Exp. Mar. Biol. Ecol.* **337**, 178–189 (2006).
20. Hillman, J. R., Lundquist, C. J., Pilditch, C. A. & Thrush, S. F. The role of large macrofauna in mediating sediment erodibility across sedimentary habitats. *Limnol. Oceanogr.* **65**, 683–693 (2020).
21. Shi, B. *et al.* Influence of macrobenthos (*Meretrix meretrix* linnaeus) on erosion-accretion processes in intertidal flats: A case study from a cultivation zone. *J. Geophys. Res. Biogeosci.* **125**, 1–15 (2020).
22. Kristensen, E., Delefosse, M., Quintana, C. O., Flindt, M. R. & Valdemarsen, T. Influence of benthic macrofauna community shifts on ecosystem functioning in shallow estuaries. *Front. Mar. Sci.* **1**, 1–14 (2014).
23. Shull, D. H., Benoit, J. M., Wojcik, C. & Senning, J. R. Infaunal burrow ventilation and pore-water transport in muddy sediments. *Estuar. Coast. Shelf Sci.* **83**, 277–286 (2009).
24. Coppock, R. L. *et al.* Benthic fauna contribute to microplastic sequestration in coastal sediments. *J. Hazard. Mater.* **415**, 125583 (2021).
25. Norkko, A., Villnäs, A., Norkko, J., Valanko, S. & Pilditch, C. Size matters: Implications of the loss of large individuals for ecosystem function. *Sci. Rep.* **3**, 1–8 (2013).
26. Gammal, J., Norkko, J., Pilditch, C. A. & Norkko, A. Coastal hypoxia and the importance of benthic macrofauna communities for ecosystem functioning. *Estuar. Coasts* **40**, 457–468 (2017).
27. Hillman, J. R., Lundquist, C. J., O'Meara, T. A. & Thrush, S. F. loss of large animals differentially influences nutrient fluxes across a heterogeneous marine intertidal soft-sediment ecosystem. *Ecosystems* **24**, 272–283 (2020).
28. Ladewig, S. M., Bianchi, T. S., Coco, G., Hope, J. A. & Thrush, S. F. A call to evaluate plastic's impacts on marine benthic ecosystem interaction networks. *Environ. Pollut.* **273**, 116423 (2021).
29. Hope, J. A., Coco, G., Parsons, D. M. & Thrush, S. F. Microplastics interact with benthic biostabilization processes. *J. Phys. Energy* **2**, 1–31 (2020).
30. Van Prooijen, B. C., Montserrat, F. & Herman, P. M. J. A process-based model for erosion of *Macoma balthica*-affected mud beds. *Cont. Shelf Res.* **31**, 527–538 (2011).
31. Gilbert, F., Stora, G. & Cuny, P. Functional response of an adapted subtidal macrobenthic community to an oil spill: macrobenthic structure and bioturbation activity over time throughout an 18-month field experiment. *Environ. Sci. Pollut. Res.* **22**, 15285–15293 (2015).
32. Gong, Z. & Zhang, Q. Impact of heavy metals (cadmium and copper) stress on the bioturbation potential of polychaete *Perinereis aibuhitensis* (family Nereididae). *Mar. Environ. Res.* **177**, 105621 (2022).
33. Boudreau, B. P. The mathematics of early diagenesis: From worms to waves. *Rev. Geophys.* **38**, 389–416 (2000).

34. Meysman, F. J. R., Galaktionov, O. S., Madani, S. & Middelburg, J. J. Modelling biological interactions in aquatic sediments as coupled reactive transport. *Interact. Betw. Macro- Microorg. Mar. Sedim.* https://doi.org/10.1029/CE060p0359 (2013).
35. Dunn, S. M. & Aller, R. C. Macrofaunal mucus secretions and tube linings in marine sediments. *J. Mar. Res.* **5**, 957–981 (2005).
36. Mermillod-Blondin, F., Rosenberg, R., François-Carcaillet, F., Norling, K. & Mauclaire, L. Influence of bioturbation by three benthic infaunal species on microbial communities and biogeochemical processes in marine sediment. *Aquat. Microb. Ecol.* **36**, 271–284 (2004).
37. Michaud, E., Aller, R. C. & Stora, G. Sedimentary organic matter distributions, burrowing activity, and biogeochemical cycling: Natural patterns and experimental artifacts. *Estuar. Coast. Shelf Sci.* **90**, 21–34 (2010).
38. Herbert, R. A. Nitrogen cycling in coastal marine ecosystems. *FEMS Microbiol. Rev.* **23**, 563–590 (1999).
39. Joye, S. B. & Anderson, I. C. *Nitrogen in the Marine Environment*. https://doi.org/10.1016/B978-0-12-372522-6.00019-0 (Elsevier Inc., 2008).
40. Schenone, S., O'Meara, T. A. & Thrush, S. F. Non-linear effects of macrofauna functional trait interactions on biogeochemical fluxes in marine sediments change with environmental stress. *Mar. Ecol. Prog. Ser.* **624**, 13–21 (2019).
41. Aller, R. C. & Cochran, J. K. The critical role of bioturbation for particle dynamics, priming potential, and organic c remineralization in marine sediments: Local and basin scales. *Front. Earth Sci.* **7**, 1–14 (2019).
42. Pischedda, L., Poggiale, J. C., Cuny, P. & Gilbert, F. Imaging oxygen distribution in marine sediments. The importance of bioturbation and sediment heterogeneity. *Acta Biotheor.* **56**, 123–135 (2008).
43. Welsh, D. T. It's a dirty job but someone has to do it: The role of marine benthic macrofauna in organic matter turnover and nutrient recycling to the water column. *Chem. Ecol.* **19**, 321–342 (2003).
44. Townsend, M., Thrush, S. F., Hewitt, J. E., Lohrer, A. M. & McCartain, L. Behavioural changes in the Tellinid bivalve *Macomona liliana* (Iredale, 1915) following exposure to a thin terrigenous sediment deposition event: Evidence from time-lapse photography. *Cah. Biol. Mar.* **55**, 475–483 (2014).
45. Hope, J. A., Coco, G. & Thrush, S. F. effects of polyester microfibers on microphytobenthos and sediment-dwelling infauna. *Environ. Sci. Technol.* https://doi.org/10.1021/acs.est.0c00514 (2020).
46. Thrush, S. F. *et al.* Cumulative stressors reduce the self-regulating capacity of coastal ecosystems. *Ecol. Appl.* **31**, e02223 (2021).
47. Volkenborn, N. *et al.* Intermittent bioirrigation and oxygen dynamics in permeable sediments: An experimental and modeling study of three tellinid bivalves. *J. Mar. Res.* **70**, 794–823 (2012).
48. Mazik, K. & Elliott, M. The effects of chemical pollution on the bioturbation potential of estuarine intertidal mudflats. *Helgol. Mar. Res.* **54**, 99–109 (2000).
49. Thrush, S. F., Hewitt, J. E., Gibbs, M., Lundquist, C. & Norkko, A. Functional role of large organisms in intertidal communities: Community effects and ecosystem function. *Ecosystems* **9**, 1029–1040 (2006).
50. Kauppi, L. *et al.* Changes in macrofauna bioturbation during repeated heatwaves mediate changes in biogeochemical cycling of nutrients. *Front. Mar. Sci.* **9**, 1–13 (2023).
51. Vlaminck, E., Cepeda, E., Moens, T. & Van Colen, C. Ocean acidification modifies behaviour of shelf seabed macrofauna: A laboratory study on two ecosystem engineers, *Abra alba* and *Lanice conchilega*. *J. Exp. Mar. Biol. Ecol.* **558**, 151831 (2023).
52. Siwicka, E., Thrush, S. F. & Hewitt, J. E. Linking changes in species–trait relationships and ecosystem function using a network analysis of traits. *Ecol. Appl.* **30**, 1–10 (2020).
53. Schenone, S. & Thrush, S. F. Unraveling ecosystem functioning in intertidal soft sediments: the role of density-driven interactions. *Sci. Rep.* **10**, 1–9 (2020).
54. Hope, J. A., Coco, G., Ladewig, S. M. & Thrush, S. F. The distribution and ecological effects of microplastics in an estuarine ecosystem. *Environ. Pollut.* **288**, 117731 (2021).
55. Zhou, Z. *et al.* Vertical microplastic distribution in sediments of Fuhe River estuary to Baiyangdian Wetland in Northern China. *Chemosphere* **280**, 130800 (2021).
56. Bermúdez, M. *et al.* Unravelling spatio-temporal patterns of suspended microplastic concentration in the Natura 2000 Guadalquivir estuary (SW Spain): Observations and model simulations. *Mar. Pollut. Bull.* **170**, 112622 (2021).
57. Chen, Z., Bowen, M., Li, G., Coco, G. & Hall, B. Retention and dispersion of buoyant plastic debris in a well-mixed estuary from drifter observations. *Mar. Pollut. Bull.* **180**, 113793 (2022).
58. Sadri, S. S. & Thompson, R. C. On the quantity and composition of floating plastic debris entering and leaving the Tamar Estuary, Southwest England. *Mar. Pollut. Bull.* **81**, 55–60 (2014).
59. Carson, H. S., Colbert, S. L., Kaylor, M. J. & McDermid, K. J. Small plastic debris changes water movement and heat transfer through beach sediments. *Mar. Pollut. Bull.* **62**, 1708–1713 (2011).
60. Ladewig, S. M., Coco, G., Hope, J. A., Vieillard, A. M. & Thrush, S. F. Real-world impacts of microplastic pollution on sea floor ecosystem function. *Sci. Total Environ.* **858**, 160114 (2023).
61. Rosenberg, R., Nilsson, H. C. & Diaz, R. J. Response of benthic fauna and changing sediment redox profiles over a hypoxic gradient. *Estuar. Coast. Shelf Sci.* **53**, 343–350 (2001).
62. Yu, L. *et al.* Modeling the role of riverine organic matter in hypoxia formation within the coastal transition zone off the Pearl River Estuary. *Limnol. Oceanogr.* **66**, 452–468 (2021).
63. Morris, J. T. & Bradley, P. M. Effects of nutrient loading on the carbon balance of coastal wetland sediments. *Limnol. Oceanogr.* **44**, 699–702 (1999).
64. Paerl, H. W. Assessing and managing nutrient-enhanced eutrophication in estuarine and coastal waters: Interactive effects of human and climatic perturbations. *Ecol. Eng.* **26**, 40–54 (2006).
65. Schenone, S. *et al.* Mapping the delivery of ecological functions combining field collected data and unmanned aerial vehicles (UAVs). *Ecosystems* https://doi.org/10.1007/s10021-021-00694-w (2021).
66. Volkenborn, N., Hedtkamp, S. I. C., van Beusekom, J. E. E. & Reise, K. Effects of bioturbation and bioirrigation by lugworms (*Arenicola marina*) on physical and chemical sediment properties and implications for intertidal habitat succession. *Estuar. Coast. Shelf Sci.* **74**, 331–343 (2007).
67. Middelburg, J. J. & Levin, L. A. Coastal hypoxia and sediment biogeochemistry. *Biogeosciences* **6**, 1273–1293 (2009).
68. Volkenborn, N., Polerecky, L., Wethey, D. S., DeWitt, T. H. & Woodin, S. A. Hydraulic activities by ghost shrimp *Neotrypaea californiensis* induce oxic-anoxic oscillations in sediments. *Mar. Ecol. Prog. Ser.* **455**, 141–156 (2012).
69. Woodin, S. A. *et al.* Same pattern, different mechanism: Locking onto the role of key species in seafloor ecosystem process. *Sci. Rep.* **6**, 1–11 (2016).
70. Michels, J., Stippkugel, A., Lenz, M., Wirtz, K. & Engel, A. Rapid aggregation of biofilm-covered microplastics with marine biogenic particles. *Proc. R. Soc. B Biol. Sci.* **285**, 20181203 (2018).
71. Rogers, K. L., Carreres-Calabuig, J. A., Gorokhova, E. & Posth, N. R. Micro-by-micro interactions: How microorganisms influence the fate of marine microplastics. *Limnol. Oceanogr. Lett.* **5**, 18–36 (2020).
72. Seeley, M. E., Song, B., Passie, R. & Hale, R. C. Microplastics affect sedimentary microbial communities and nitrogen cycling. *Nat. Commun.* **11**, 1–10 (2020).
73. Glud, R. N. Oxygen dynamics of marine sediments. *Mar. Biol. Res.* **4**, 243–289 (2008).
74. Vieillard, A. M. & Thrush, S. F. Ecogeochemistry and denitrification in non-eutrophic coastal sediments. *Estuar. Coasts* **44**, 1866–1882 (2021).

75. Shang, H. A generic hierarchical model of organic matter degradation and preservation in aquatic systems. *Commun. Earth Environ.* **4**, 1–10 (2023).
76. Archer, D. E., Morford, J. L. & Emerson, S. R. A model of suboxic sedimentary diagenesis suitable for automatic tuning and gridded global domains. *Global Biogeochem. Cycles* **16**, 171–1721 (2002).
77. Boudreau, B. P. *Diagenetic Models and Their Implementation: Modelling Transport and Reactions in Aquatic Sediments* (Springer, 1996).
78. Middelburg, J. J., Soetaert, K. & Herman, P. M. J. Empirical relationships for use in global diagenetic models. *Deep. Res. Part I Oceanogr. Res. Pap.* **44**, 327–344 (1997).
79. Fazey, F. M. C. & Ryan, P. G. Biofouling on buoyant marine plastics: An experimental study into the effect of size on surface longevity. *Environ. Pollut.* **210**, 354–360 (2016).
80. Hailes, S. F. & Hewitt, J. E. *Manukau Harbour Ecological Monitoring Programme : Report on Data Collected up Until February 2007*. Vol. 4525 (2007).
81. Maire, O., Duchêne, J. C., Bigot, L. & Grémare, A. Linking feeding activity and sediment reworking in the deposit-feeding bivalve *Abra ovata* with image analysis, laser telemetry, and luminophore tracers. *Mar. Ecol. Prog. Ser.* **351**, 139–150 (2007).
82. Masura, J., Baker, J., Foster, G. & Arthur, C. *Laboratory Methods for the Analysis of Microplastics in the Marine Environment: Recommendations for Quantifying Synthetic Particles in Waters and Sediments*. (NOAA Technical Memorandum NOS-OR&R-48, 2015).
83. Bernard, G. *et al.* Experimental assessment of the effects of temperature and food availability on particle mixing by the bivalve abra alba using new image analysis techniques. *PLoS One* **11**, 1–23 (2016).
84. Gerino, M. *et al.* Comparison of different tracers and methods used to quantify bioturbation during a spring bloom: 234-thorium, luminophores and chlorophyll a. *Estuar. Coast. Shelf Sci.* **46**, 531–547 (1998).
85. Crank, J. *The Mathematics of Diffusion* (Oxford University Press, 1975).
86. Van Kessel, J. F. The relation between redox potential and denitrification in a water-sediment system. *Water Res.* **12**, 285–290 (1978).

Acknowledgements

We thank Ocean Change II project for research support. We appreciate the support from seafloor ecology team and staff in Leigh Marine laboratory, the University of Auckland.

Author contributions

Y.Y. led the project, designed and ran the experiment and the laboratory analysis and analysed the data. S.F.T. and A.D.P. supervised the project and provided consultancy for experimental design and statistical analysis. Y.Y. led the writing of the manuscript. S.F.T. and A.D.P. contributed to the writing and the revision of the manuscript.

Competing interests

The authors declare no competing interests.

Additional information

Supplementary Information The online version contains supplementary material available at https://doi.org/10.1038/s41598-023-44425-8.

Correspondence and requests for materials should be addressed to Y.Y.

Reprints and permissions information is available at www.nature.com/reprints.

Publisher's note Springer Nature remains neutral with regard to jurisdictional claims in published maps and institutional affiliations.